

University of Nebraska - Lincoln

DigitalCommons@University of Nebraska - Lincoln

---

Mechanical & Materials Engineering Faculty  
Publications

Mechanical & Materials Engineering, Department  
of

---

10-2016

# Thermal analysis of continuous and patterned multilayer films in the presence of a nanoscale hot spot


Jia-Yang Juang

*National Taiwan University, jiaayang@ntu.edu.tw*

Jinglin Zheng

*University of Nebraska-Lincoln, jinglin.zheng@unl.edu*

Follow this and additional works at: <http://digitalcommons.unl.edu/mechengfacpub>

 Part of the [Mechanics of Materials Commons](#), [Nanoscience and Nanotechnology Commons](#), [Other Engineering Science and Materials Commons](#), and the [Other Mechanical Engineering Commons](#)

---

Juang, Jia-Yang and Zheng, Jinglin, "Thermal analysis of continuous and patterned multilayer films in the presence of a nanoscale hot spot" (2016). *Mechanical & Materials Engineering Faculty Publications*. 167.

<http://digitalcommons.unl.edu/mechengfacpub/167>

This Article is brought to you for free and open access by the Mechanical & Materials Engineering, Department of at DigitalCommons@University of Nebraska - Lincoln. It has been accepted for inclusion in Mechanical & Materials Engineering Faculty Publications by an authorized administrator of DigitalCommons@University of Nebraska - Lincoln.

## Thermal analysis of continuous and patterned multilayer films in the presence of a nanoscale hot spot

Jia-Yang Juang (莊嘉揚)<sup>1,a</sup> and Jinglin Zheng (郑静琳)<sup>2</sup>

<sup>1</sup>Department of Mechanical Engineering, National Taiwan University, Taipei 10617, Taiwan

<sup>2</sup>Department of Mechanical and Materials Engineering, University of Nebraska at Lincoln, Lincoln, Nebraska 68588, USA

(Received 1 September 2016; accepted 26 September 2016; published online 3 October 2016)

Thermal responses of multilayer films play essential roles in state-of-the-art electronic systems, such as photo/micro-electronic devices, data storage systems, and silicon-on-insulator transistors. In this paper, we focus on the thermal aspects of multilayer films in the presence of a nanoscale hot spot induced by near field laser heating. The problem is set up in the scenario of heat assisted magnetic recording (HAMR), the next-generation technology to overcome the data storage density limit imposed by superparamagnetism. We characterized thermal responses of both continuous and patterned multilayer media films using transient thermal modeling. We observed that material configurations, in particular, the thermal barriers at the material layer interfaces crucially impact the temperature field hence play a key role in determining the hot spot geometry, transient response and power consumption. With a representative generic media model, we further explored the possibility of optimizing thermal performances by designing layers of heat sink and thermal barrier. The modeling approach demonstrates an effective way to characterize thermal behaviors of micro and nano-scale electronic devices with multilayer thin film structures. The insights into the thermal transport scheme will be critical for design and operations of such electronic devices. © 2016 Author(s). All article content, except where otherwise noted, is licensed under a Creative Commons Attribution (CC BY) license (<http://creativecommons.org/licenses/by/4.0/>). [<http://dx.doi.org/10.1063/1.4964497>]

### I. INTRODUCTION

Multilayer films play essential roles in state-of-the-art electronic systems, such as photo/micro-electronic devices, data storage systems, and silicon-on-insulator transistors. For instance, the rapid growth of hard disk drive areal density over the decades is realized by shrinking down the size of individual magnetic bit on the storage media featuring a multilayer film structure. However, the data bit down-sizing is now reaching a limit set by superparamagnetism: the magnetization of the sufficiently small data bit can randomly flip direction under the influence of temperature.<sup>1</sup> One way to maintain thermal stability with smaller bit size is to take advantage of the temperature dependence of anisotropy energy density. It is known that anisotropy energy of ferromagnetic materials falls toward zero when temperature rises toward the Curie Temperature  $T_c$ . Thus a recording material with high anisotropy and small grains will be capable of circumvent superparamagnetism if we can heat it beyond  $T_c$  temporarily during writing and cool it off immediately after writing. Today under active development is the so-called heat-assisted-magnetic-recording (HAMR),<sup>2-5</sup> which uses a laser focused by a near field transducer (NFT) to locally heat a storage media placed in proximity. Alternatively, patterning the media as composed of isolated magnetic islands using lithography is another possible solution to maintain bit thermal stability with even a moderate anisotropy energy density.<sup>6-9</sup> With this type of media, termed as bit patterned media (BPM), the requirement on a strong writing field is relaxed. Although HAMR and BPM are different in nature and have their own gating

<sup>a</sup>Electronic mail: [jiayang@ntu.edu.tw](mailto:jiayang@ntu.edu.tw).

factors towards commercialization, they are compatible with each other and their combination owns the potential to push the areal density to an ultimate limit. Recently it is demonstrated that an areal density of 1 Tb/in<sup>2</sup> is achieved by combining these two technologies.<sup>10</sup> In this case, BPM relaxes HAMR's demand on small-grain materials and HAMR makes it unnecessary to scale down the writer width in BPM.

However, data writing in a HAMR system relies heavily on accomplishment of a desirable media temperature profile. Yet the system's complicated nature prohibits direct measurements of such profiles.<sup>11,12</sup> On the other hand, numerical modeling provides a viable way to characterize media thermal responses and provide guidelines for experiments.<sup>13-17</sup> In these studies, laser heating is treated either as flux boundary conditions at the surface or as absorbed power determined by the Maxwell equation, with only the latter capturing the physics of energy propagation in the multilayer films. Temperature profiles are solved based on either the continuum Fourier equation or Boltzmann transport equation. Although the latter captures temperature slips at interfaces, the computational efforts to accommodate multiple layers with different length scales with a sub-continuum model are tremendous. In this study we introduced interface thermal conductance based on empirical data into the continuum-based model to capture interface temperature jumps. How material and geometry configurations impact the multilayer's thermal performances are demonstrated by a side-by-side comparison of three representative media in HAMR. We find that thermal barriers at material interfaces play an essential role in determining key parameters like the hot spot size, time constants and power consumption. Using a generic model, we further explored performance optimization with heat sink and thermal barrier designs. This model demonstrates an effective approach to characterize thermal behaviors of micro and nano-scale electronic devices with multilayer films. The insights into various thermal aspects will be critical for design and operations of such devices.

## II. NUMERICAL MODELING

We focus on three representative multilayer configurations in HAMR: continuous CoPd media (CoPd), bit patterned CoPd media (BPM), and continuous FePt media (FePt).<sup>18-22</sup> Figures 1(a)-(c) show the schematics of media structures. In particular, BPM has exactly the same material configuration as CoPd except that it consists of regularly spaced isolated islands (24 nm × 24 nm) with a pitch of 36 nm and a height of 16 nm. Thus the comparison between CoPd and BPM reveals the impact of geometry discontinuity. Both CoPd and FePt are continuous hence their comparison shows the effects of material configuration.

Transient finite element analysis is used to solve the heat equation. To capture temperature slips at interfaces, contact elements are applied at material boundaries with empirical thermal conductance  $50 \times 10^8$  W/(m<sup>2</sup>·K) at metal/metal interfaces,  $1 \times 10^8$  W/(m<sup>2</sup>·K) at metal/SiO<sub>2</sub> interfaces and  $7 \times 10^8$  W/(m<sup>2</sup>·K) at metal/MgO interfaces.<sup>23</sup> Other material properties are listed in Table I. Material anisotropy is taken into account, assuming out-of-plane and in-plane thermal conductivity ratio is 2 for CoPd and 5 for FePt.<sup>24</sup> As shown in Fig. 1(d), the model is sized at 3 μm × 1.5 μm × 0.6 μm in down-track (x), cross-track (y) and thickness (z) directions, respectively. Only half of the media is modeled in the cross-track direction to take advantage of the symmetry. Dirichlet boundary condition ( $T = 0$  °C) is applied at all boundaries except for the symmetry plane, which is a reasonable assumption considering the spot size (~50 nm) and the temperature elevation (~600 °C). The laser power absorption profiles are extracted from electro-magnetic simulations, assuming 6 nm head-media spacing,<sup>10,16,21</sup> and applied as heat generation rate in the model. The approach has demonstrated good correlations with Full Width at Half Maximum (FWHM) measurements.<sup>21</sup>

## III. RESULTS AND DISCUSSIONS

Figures 2(a)-(c) show the three media's temperature fields when surface temperature maximum reaches 600 °C. The power consumption is 0.96, 0.36 and 0.32 mW for CoPd, BPM and FePt, respectively. Models are cut open at the location right beneath NFT. CoPd features the largest hot spot, whereas in BPM heat is mostly concentrated on the island, showing that a patterned surface increases thermal efficiency which is consistent with previous studies.<sup>22</sup>

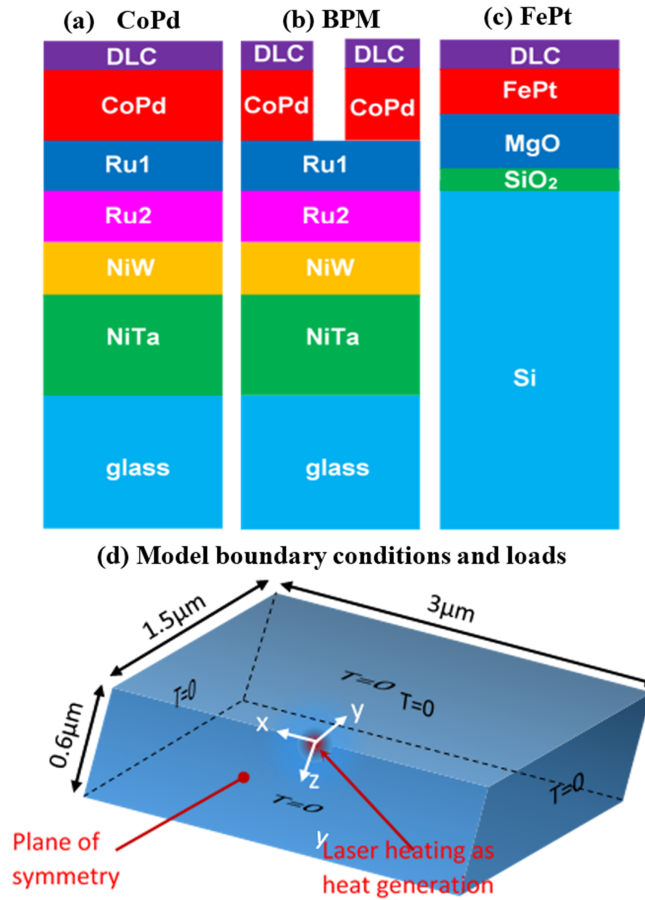


FIG. 1. Schematics of media configuration: (a) CoPd, (b) BPM, (c) FePt, and (d) boundary conditions and loads.

TABLE I. Material properties of multilayers.

	Density ( $\times 10^3$ kg/m <sup>3</sup> )	Specific heat ( $\times 10^3$ J/kg/K)	Thermal conductivity (W/m/K)
DLC	1.9	0.57	1.3
CoPd	7.9	0.42	10( $\perp$ ), 5(=) <sup>a</sup>
Ru2	12.3	0.23	45
Ru1	12.3	0.23	68
NiW	8.9	0.42	9.8
NiTa	8.7	0.42	7.7
Glass	2.51	0.753	1.12
FePt	13.21	0.37	10( $\perp$ ), 2(=)
MgO	3.58	0.877	4
SiO <sub>2</sub>	2.196	0.74	1
Si	2.33	0.702	148

<sup>a</sup>( $\perp$ ) means out-of-plane thermal conductivity and (=) means in-plane thermal conductivity.

Cross-section temperature profiles in Figs 2(d)-(f) reveal more details. BPM's spot size is dominated by the island dimension which is 24 nm. For the other two continuous media, CoPd shows a narrower peak in both down-track and cross-track directions, but the profile spreads out quickly as the temperature falls below 200 °C. In practice, we use FWHM, defined as cross-track width of the profile at half of the peak temperature, to characterize the achievable track width, (Fig. 2(e) illustrates FWHM for CoPd). In that sense, CoPd has an FWHM of 54 nm, smaller compared to FePt's 78 nm

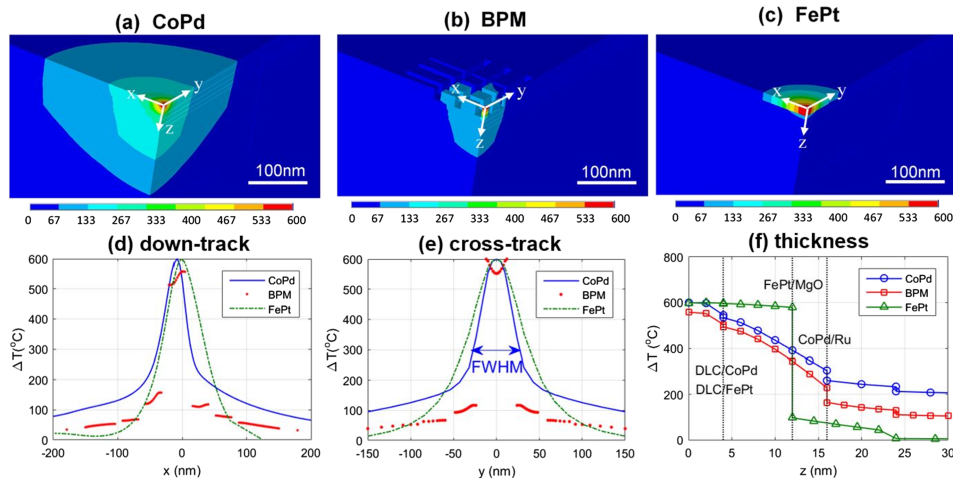


FIG. 2. Temperature fields of CoPd, BPM and FePt when surface temperature maximum reaches 600 °C. (a)-(c) compare the 3-D temperature fields cut open at the media location right beneath NFT. (d)-(f) show temperature profiles along down-track, cross-track and thickness directions, respectively.

despite an overall larger spot. Figure 2(f) shows temperature profiles along z axis. FePt shows a flat profile from overcoat to the recording layer (RL) followed by a jump of nearly 500 °C at FePt/MgO interface, resulting in little heat spreading beyond RL.

It is more relevant to look at the recording layer temperature because this is where writing happens. Figures 3(a) shows the cross-track temperature profiles at the middle of the recording layer when

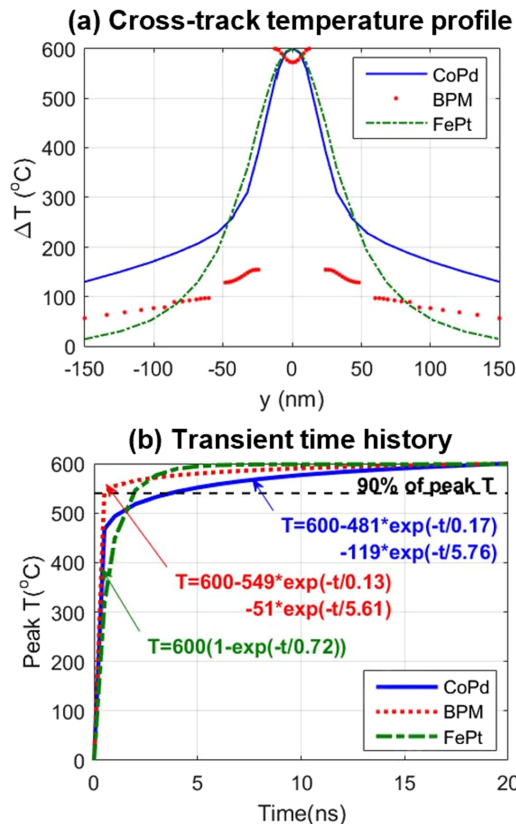


FIG. 3. Thermal responses when peak  $T_{RL}$  reaches 600 °C (a) cross-track  $T_{RL}$  (b) transient time history.

maximum  $T_{RL}$  reaches 600 °C. In this case, the power consumption is 1.32, 0.52 and 0.32 mW for CoPd, BPM and FePt, respectively. CoPd's FWHM increases to 68 nm, showing a strong sensitivity to power, whereas FePt's FWHM and power consumption almost remain unaffected.

Another interesting characteristic is how soon a steady hot spot can be formed once the laser is on. For multilayers, a characteristic thermal time constant can be calculated from material properties and characteristic length.<sup>25</sup> As shown in Fig. 3(b), responses of CoPd and BPM are characterized by two-term exponential rises, with a first term arising from thin magnetic and inter-layers and a second term contributed by thick under-layers like NiTa. On the other hand, FePt's response is dominated by the time constant of MgO layer. If we use the time taken to reach 90% of the peak temperature to quantify the media's transient performance, the response time is 3.7, 0.5, 1.9 ns for CoPd, BPM and FePt, respectively. BPM excels due to the dominance of its first exponential term despite its slowness at the tail of the curve. FePt follows benefitting from its material configuration.

Above simulations are all conducted assuming no disk-spinning, which is not the real case. Disk spinning spreads heat in the down-track direction and this effect is non-negligible in a conventional perpendicular recording system with thermal flying-height control.<sup>26</sup> The same mechanism exists in HAMR. Here we vary the disk linear speed from 0 m/s to 32 m/s and observe temperature changes given the same power absorption. If we define width of the profile at the half magnitude (Fig. 4(a)) as the spot's down-track size, the spot stretches by 25% when the disk speed increases from 0 to 32 m/s, as shown in Fig. 4(b). In the meantime, the maximum  $T_{RL}$  reduces by 20%.

HAMR performance is contingent on coordination of all the magnetic, thermal and mechanical aspects. Recording media with a tight FWHM, power efficiency, faster response and uniform  $T_{RL}$  is always in favor. This involves how to configure the media to achieve the best trade-offs among these aspects. One effective strategy is to manage heat propagation using heat sinks and thermal barriers. Here we start from a generic FePt media with a Cu heat sink layer below the recording layer and a thermal barrier between the heat sink and recording layer, as shown in Fig. 5(a). Then we tweak Cu thickness  $t$  and modify the interface thermal conductance  $C$  between Cu and FePt to see how the thermal response varies. Figure 5(b) shows contour of power consumption when maximum  $T_{RL}$  reaches 600 °C. A thin heat sink layer with lower interface conductance is in favor and interface conductance dominates. But this has to trade off with a small FWHM and a fast response: as indicated by Figs. 5(c) and 5(d), a thick heat sink with high interface conductance decreases

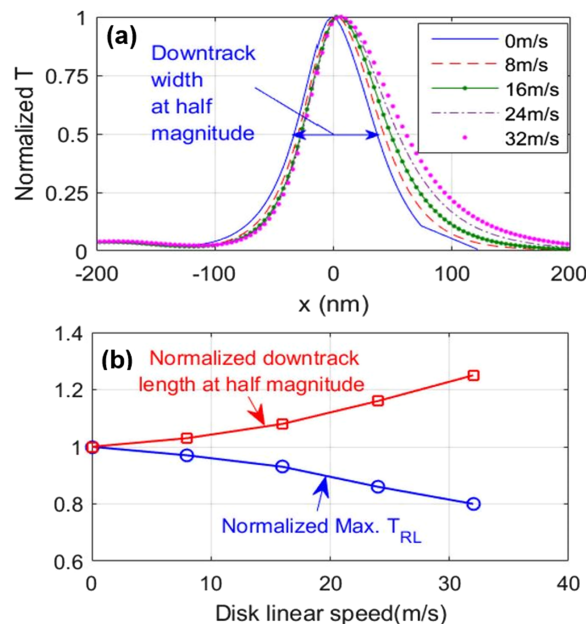


FIG. 4. Effect of linear speed (a) down-track normalized  $T_{RL}$  (b) Peak temperature decrease and down-track spot size increase with linear speed.

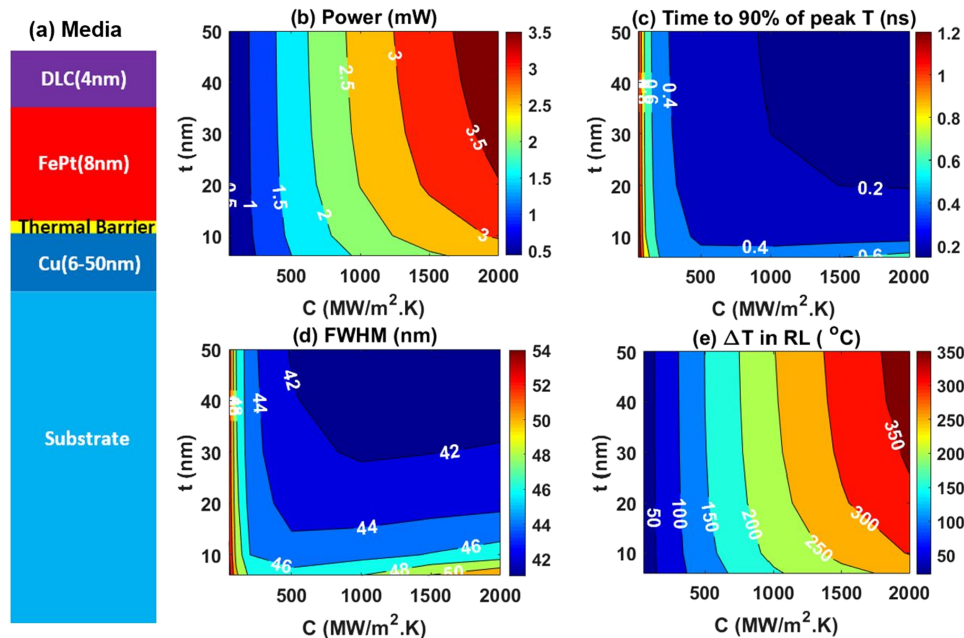


FIG. 5. Thermal figures of merit (a) generic media structure (b) power consumption for maximum  $T_{RL}$  to reach  $600\text{ }^{\circ}\text{C}$  (c) time taken to reach 90% of the peak temperature (d) cross-track FWHM at the middle of the recording layer (e)  $\Delta T$  between the top and bottom of the recording layer.

FWHM and response time. Another figure of merit is a uniform  $T_{RL}$  across the recording layer, which we use  $\Delta T$  between the top and bottom of the recording layer to characterize. As indicated by Fig. 5(e), a thin heat sink and a small interface conductance reduces temperature difference across the recording layer and again interface conductance is overwhelming. These results come in handy when we optimize the performance with certain restrictions. For instance, given an interface conductance of around  $1000\text{ MW}/(\text{m}^2\cdot\text{K})$ , we can achieve a fast response and small FWHM with comparable power efficiency and uniform  $T_{RL}$  by increasing heat sink thickness.

#### IV. CONCLUSION

We characterized thermal responses of three representative multilayer media using transient thermal modeling and found that thermal barriers at material interfaces play a significant role in determining temperature profiles. The thermal barrier between FePt and MgO significantly benefits FePt media in terms of power efficiency and FWHM sensitivity. Furthermore, geometry discontinuity raises thermal efficiency and improves time constants. With a generic FePt media we demonstrated that optimization can be accomplished with heat sink and thermal barrier designs. Our modeling approach is effective to characterize thermal behaviors of micro and nano-scale electronic devices with multilayer film structures and the results provide critical insights into design and operations of such devices.

#### ACKNOWLEDGMENTS

This work is partially supported by the Ministry of Science of Technology (MOST) of Taiwan (104-2221-E-002-024-MY2). We thank Dr. Barry Stipe for helpful discussion.

<sup>1</sup>T. W. McDaniel, *J. Phys. Condens. Matter* **17**, R315 (2005).

<sup>2</sup>R. E. Rottmayer, S. Batra, D. Buechel, W. A. Challener, J. Hohlfeld, Y. Kubota, L. L. Li, B. L. Bin Lu, C. Mihalcea, K. Mountfield, K. Pelhos, C. P. C. Peng, T. Rausch, M. A. Seigler, D. Weller, and X. Y. X. Yang, *IEEE Trans. Magn.* **42**, 2417 (2006).

<sup>3</sup>L. Pan and D. B. Bogy, *Nat. Photonics* **3**, 189 (2009).

- <sup>4</sup> W. A. Challener, C. Peng, A. V. Itagi, D. Karns, W. Peng, Y. Peng, X. Yang, X. Zhu, N. J. Gokemeijer, Y.-T. Hsia, G. Ju, R. E. Rottmayer, M. A. Seigler, and E. C. Gage, *Nat. Photonics* **3**, 303 (2009).
- <sup>5</sup> B. Marchon, X. C. Guo, B. K. Pathem, F. Rose, Q. Dai, N. Feliss, E. Schreck, J. Reiner, O. Mosendz, K. Takano, H. Do, J. Burns, and Y. Saito, *IEEE Trans. Magn.* **50**, 137 (2014).
- <sup>6</sup> H. J. Richter, A. Y. Dobin, R. T. Lynch, D. Weller, R. M. Brockie, O. Heinonen, K. Z. Gao, J. Xue, R. J. M. V. D. Veerdonk, P. Asselin, and M. F. Erden, *Appl. Phys. Lett.* **88**, 7 (2006).
- <sup>7</sup> M. Albrecht, C. T. Rettner, A. Moser, M. E. Best, and B. D. Terris, *Appl. Phys. Lett.* **81**, 2875 (2002).
- <sup>8</sup> L. Li and D. B. Bogy, *Microsyst. Technol.* **17**, 805 (2011).
- <sup>9</sup> J. Yang, J. Wei, W. Kuan, and T. Lin, 1745 (2014).
- <sup>10</sup> B. C. Stipe, T. C. Strand, C. C. Poon, H. Balamane, T. D. Boone, J. A. Katine, J.-L. Li, V. Rawat, H. Nemoto, A. Hirotsune, O. Hellwig, R. Ruiz, E. Dobisz, D. S. Kercher, N. Robertson, T. R. Albrecht, and B. D. Terris, *Nat. Photonics* **4**, 484 (2010).
- <sup>11</sup> S. Xiong and D. B. Bogy, *IEEE Trans. Magn.* **50**, 1 (2014).
- <sup>12</sup> H. Wu, S. Xiong, S. Canchi, E. Schreck, and D. Bogy, *Appl. Phys. Lett.* **108**, 093106 (2016).
- <sup>13</sup> L. Wu, 215702 (n.d.).
- <sup>14</sup> L. Wu and F. E. Talke, *Microsyst. Technol.* **17**, 1109 (2011).
- <sup>15</sup> P. Yu, W. Zhou, S. Yu, and K. S. Myo, *Microsyst. Technol.* **19**, 1457 (2013).
- <sup>16</sup> L. Huang, B. Stipe, M. Staffaroni, J. Y. Juang, T. Hirano, E. Schreck, and F. Y. Huang, *IEEE Trans. Magn.* **49**, 2565 (2013).
- <sup>17</sup> S. S. Ghai, W. T. Kim, C. H. Amon, and M. S. Jhon, *J. Appl. Phys.* **99** (2006).
- <sup>18</sup> O. Hellwig, T. Hauet, T. Thomson, E. Dobisz, J. D. Risner-Jamtegaard, D. Yaney, B. D. Terris, and E. E. Fullerton, *Appl. Phys. Lett.* **95**, 7 (2009).
- <sup>19</sup> R. Sbiaa, C. Z. Hua, S. N. Piramanayagam, R. Law, K. O. Aung, and N. Thiyagarajah, *J. Appl. Phys.* **106** (2009).
- <sup>20</sup> Y. Nozaki, N. Narita, T. Tanaka, and K. Matsuyama, *Appl. Phys. Lett.* **95**, 93 (2009).
- <sup>21</sup> L. Zhang, Y. K. Takahashi, K. Hono, B. C. Stipe, J. Y. Juang, and M. Grobis, *J. Appl. Phys.* **109**, 23 (2011).
- <sup>22</sup> K. Sendur and W. Challener, *Appl. Phys. Lett.* **94**, 2009 (2009).
- <sup>23</sup> D. G. Cahill, K. E. Goodson, and A. Majumdar, *J. Heat Transfer* **124**, 223 (2002).
- <sup>24</sup> H. Ho, A. A. Sharma, W. L. Ong, J. A. Malen, J. A. Bain, and J. G. Zhu, *Appl. Phys. Lett.* **103**, 3 (2013).
- <sup>25</sup> S. Xiong, R. Smith, N. Wang, D. Li, E. Schreck, S. Canchi, and Q. Dai, in Proceedings of the ASME 2016 Conference on Information Storage and Processing Systems, Santa Clara, California, US, 20 June - 21 June 2016.
- <sup>26</sup> J. Zheng, Y. Chen, and Q. Zhou, 1 (2016), Manuscript submitted for publication.